

# University of Groningen



# Critical role for iron accumulation in the pathogenesis of fibrotic lung disease

Ali, Md Khadem; Kim, Richard Y; Brown, Alexandra C; Donovan, Chantal; Vanka, Kanth S; Mayall, Jemma R; Liu, Gang; Pillar, Amber L; Jones-Freeman, Bernadette; Xenaki, Dikaia

Published in: JOURNAL OF PATHOLOGY

DOI: 10.1002/path.5401

IMPORTANT NOTE: You are advised to consult the publisher's version (publisher's PDF) if you wish to cite from it. Please check the document version below.

Document Version Final author's version (accepted by publisher, after peer review)

Publication date: 2020

Link to publication in University of Groningen/UMCG research database

Citation for published version (APA):

Ali, M. K., Kim, R. Y., Brown, A. C., Donovan, C., Vanka, K. S., Mayall, J. R., Liu, G., Pillar, A. L., Jones-Freeman, B., Xenaki, D., Borghuis, T., Karim, R., Pinkerton, J. W., Aryal, R., Heidari, M., Martin, K. L., Burgess, J. K., Oliver, B. G., Trinder, D., ... Horvat, J. C. (2020). Critical role for iron accumulation in the pathogenesis of fibrotic lung disease. *JOURNAL OF PATHOLOGY*, *251*(1), 49-62. https://doi.org/10.1002/path.5401

Copyright Other than for strictly personal use, it is not permitted to download or to forward/distribute the text or part of it without the consent of the author(s) and/or copyright holder(s), unless the work is under an open content license (like Creative Commons).

The publication may also be distributed here under the terms of Article 25fa of the Dutch Copyright Act, indicated by the "Taverne" license. More information can be found on the University of Groningen website: https://www.rug.nl/library/open-access/self-archiving-pure/taverneamendment.

### Take-down policy

If you believe that this document breaches copyright please contact us providing details, and we will remove access to the work immediately and investigate your claim.

Downloaded from the University of Groningen/UMCG research database (Pure): http://www.rug.nl/research/portal. For technical reasons the number of authors shown on this cover page is limited to 10 maximum.

# The Journal of Pathology, ORIGINAL PAPER

# Critical role for iron accumulation in the pathogenesis of fibrotic lung disease

Md Khadem Ali<sup>1,2</sup>, Richard Y. Kim<sup>2, 3</sup>, Alexandra C. Brown<sup>2</sup>, Chantal Donovan<sup>2,3</sup>, Kanth S. Vanka<sup>2</sup>, Jemma R. Mayall<sup>2</sup>, Gang Liu<sup>2,3</sup>, Amber L. Pillar<sup>2</sup>, Bernadette Jones-Freeman<sup>2</sup>, Dikaia Xenaki<sup>4</sup>, Theo Borghuis<sup>5</sup>, Rafia Karim<sup>2</sup>, James W. Pinkerton<sup>2,6</sup>, Ritambhara Aryal<sup>2,7</sup>, Moones Heidari<sup>7</sup>, Kristy L. Martin<sup>2,7</sup>, Janette K. Burgess<sup>4,5</sup>, Brian G. Oliver<sup>4</sup>, Debbie Trinder<sup>8</sup>, Daniel M. Johnstone<sup>9</sup>, Elizabeth A. Milward<sup>7</sup>, Philip M. Hansbro<sup>2, 3</sup><sup>†</sup> and Jay C. Horvat<sup>2,\*</sup> <sup>†</sup>

<sup>1</sup>Division of Pulmonary and Critical Care Medicine, School of Medicine, Stanford University, Stanford, USA. <sup>2</sup>Priority Research Centre for Healthy Lungs and School of Biomedical Sciences and Pharmacy and Hunter Medical Research Institute, University of Newcastle, Newcastle, NSW, Australia. <sup>3</sup>Centre for Inflammation, Centenary Institute and University of Technology Sydney, Sydney, New South Wales, Australia. <sup>4</sup>Woolcock Institute of Medical Research, University of Sydney and School of Life Sciences, University of Technology Sydney, Sydney, NSW, Australia. <sup>5</sup>University of Groningen, University Medical Centre Groningen, Department of Pathology and Medical Biology, Groningen Research Institute for Asthma and COPD, Groningen, Netherlands. <sup>6</sup>Respiratory Pharmacology & Toxicology Group, National Heart & Lung Institute, Imperial College London, London, United Kingdom. <sup>7</sup>Priority Research Centre for Brain and Mental Health and School of Biomedical Sciences, University of Newcastle, Newcastle, NSW, Australia. <sup>8</sup>Medical School and, Harry Perkins Institute of Medical Research, University of Western Australia, Perth, WA, Australia. <sup>9</sup>Discipline of Physiology and Bosch Institute, University of Sydney, Sydney, NSW, Australia.

# <sup>†</sup>These authors contributed equally to this manuscript

This article has been accepted for publication and undergone full peer review but has not been through the copyediting, typesetting, pagination and proofreading process which may lead to differences between this version and the Version of Record. Please cite this article as doi:10.1002/path.5401

# **Conflicts of interest**

Accepted Article

No conflicts of interest were declared.

\*Correspondence to J Horvat, Priority Research Centre for Healthy Lungs, Hunter Medical Research Institute, Lot 1 Kookaburra Circuit, New Lambton Heights, Newcastle, New South Wales, 2305, Australia. E-mail: <u>jay.horvat@newcastle.edu.au</u>

Short Running Head: Role of iron accumulation in fibrotic lung disease

# ABSTRACT

Increased iron levels and/or dysregulated iron homeostasis occurs in several lung diseases. Here, the effects of iron accumulation on the pathogenesis of pulmonary fibrosis and associated lung function decline was investigated using a combination of murine models of iron overload and bleomycin-induced pulmonary fibrosis, primary human lung fibroblasts treated with iron and histological samples from patients with or without idiopathic pulmonary fibrosis (IPF)

Iron levels are significantly increased in iron overloaded transferrin receptor 2 (Tfr2) mutant mice and homeostatic iron regulator (Hfe) gene-deficient mice and this is associated with increases in airways fibrosis and reduced lung function. Furthermore, fibrosis and lung function decline are associated with pulmonary iron accumulation in bleomycin-induced pulmonary fibrosis. We also show that iron accumulation is increased in lung sections from IPF patients and that human lung fibroblasts show greater proliferation, and cytokine and extracellular matrix responses when exposed to increased iron levels. Significantly, we show that intranasal treatment with the iron chelator, deferoxamine (DFO), from the time when pulmonary iron levels accumulate, prevents airway fibrosis and decline in lung function in experimental pulmonary fibrosis. Pulmonary fibrosis is associated with an increase in Tfr1<sup>+</sup> macrophages that display altered phenotype in disease and DFO treatment modified the abundance of these cells.

These experimental and clinical data demonstrate that increased accumulation of pulmonary iron plays a key role in the pathogenesis of pulmonary fibrosis and lung function decline. Furthermore, these data highlight the potential for the therapeutic targeting of increased pulmonary iron in the treatment of fibrotic lung diseases such as IPF.

### Abstract word count: 248 up to 300 OK

**Keywords:** Iron, pulmonary fibrosis, airway remodelling, IPF, lung function, bleomycin, airway inflammation, airway hyperresponsiveness, deferoxamine, collagen

Dysregulation of iron homeostasis is associated with a range of respiratory diseases, particularly those associated with pulmonary fibrosis (reviewed in [1]). Specifically, patients with IPF have increases in total iron levels, iron-laden macrophages, and iron-induced oxygen radical formation in the lung and recent evidence shows that iron sequestration by alveolar macrophages (AM) is defective in idiopathic pulmonary fibrosis (IPF) patients compared to healthy controls [1,2]. However, it is unknown whether altered iron regulation and level affect the progression of IPF and/or whether changes in iron homeostasis are a cause or consequence of disease.

Murine models of iron overload allow the examination of the effects of increased iron accumulation in the lung *in vivo* in the absence of disease-associated and/or -inducing stimuli that alter iron levels as a consequence of inflammation/disease [1]. Systemic iron overload results in increased iron accumulation in the lung, predominantly localized to AMs, ciliated airway epithelial cells (AEC), alveolar type II cells and/or vascular smooth muscle cells [3,4]. Significantly, iron overload in mice results in significant increases inflammatory responses and oxidative/nitrosative stress in the lungs [5] as well as oxidative stress, decreased total lung capacity and compliance, hypoxemia and increases in lung elastance [4].

Collectively, these studies support that pulmonary iron accumulation may induce pathological features associated with a number of lung diseases. However, they do not address how iron accumulation affects pulmonary fibrosis and lung function decline, specifically in fibrotic lung disease, and/or whether iron accumulation can be therapeutically targeted to prevent the progression of fibrotic lung disease. In this study, we use a complementary combination of murine models of iron overload and bleomycin-induced pulmonary fibrosis and IPF patient samples and human lung fibroblasts cultured in the presence of increased iron to demonstrate how iron accumulation plays an important role, and can be therapeutically targeted, in the pathogenesis and progression of fibrotic lung disease.

# Materials and methods

Full details are provided in supplementary material, Supplementary materials and methods.

### **Study approvals**

All animal protocols were approved by the Animal Ethics Committees of the University of Newcastle and University of Sydney, Australia. All human protocols were approved by the Human Ethics Committee of The University of Sydney and the Sydney South West Area Health Service. The study protocol was consistent with the Research Code of the University Medical Centre Groningen and Dutch national ethical and professional guidelines ("Code of conduct; Dutch federation of biomedical scientific societies"; http://www.federa.org [last accessed 09/02/2020]).

## Iron overload mice and experimental lung fibrosis

*Transferrin receptor*  $2^{Y245X}$  mutant (*Tfr2<sup>mut/mut</sup>*) [6] and hemochromatosis protein gene (*Hfe*)deficient mice (*Hfe*<sup>-/-</sup>) [7] on the AKR background strain aged 36 weeks were used to model iron overload. Bleomycin-induced experimental fibrosis was induced in *Tfr2<sup>mut/mut</sup>*, wild-type (WT) AKR aged 12 weeks , and WT BALB/c mice aged 6-8 weeks to assess the effects of iron on fibrosis [8,9]. Iron quantification [10,11], airway inflammation [12,13], small airway fibrosis [8], pulmonary tissue density, Ashcroft score quantification [14], hydroxyproline assay [8], pulmonary macrophage phenotypic characterization [15], lung function [12,13,16-20], airway contractility [21-24] and therapeutic treatment with the iron chelator DFO was assessed as previously described and/or as described in supplementary materials and methods.

## Analysis of human tissues

Iron levels in IPF patient lung tissues were assessed using 3, 3'-diaminobenzidinetetrahydrochloride (DAB)-enhanced Perls' iron staining [11,25,26]. The effect of iron accumulation on cellular proliferation, cytokine secretion and extracellular matrix (ECM) gene expression in primary human fibroblasts was assessed by MTT assay [27], ELISA [27] and RTqPCR as described previously and/or as described in supplementary materials and methods. IPF patient details are outlined in supplementary materials and methods, Table S1.

## **Statistics**

Data are presented as means ± SEM. Data were analysed using GraphPad Prism software (GraphPad Software, Inc., San Diego, CA, USA). Statistical significance between two groups was quantified using Student's two-tailed, unpaired *t*-test. Comparisons between multiple groups were performed using a one-way ANOVA with a Fisher's Least Significant Difference (LSD) *post hoc* test. Airway hyperresponsiveness (AHR) and proliferation data were analysed using two-way repeated measures ANOVA with a Bonferroni *post hoc* test.

# Results

# Iron levels and airways fibrosis are increased in the lungs of $Tfr2^{mut/mut}$ and $Hfe^{-/-}$ mice

To enable us to define the roles of increased iron in human lungs and how this affects disease features, we first assessed iron levels and airways fibrosis in the lungs of  $Tfr2^{mut/mut}$  and  $Hfe^{-f}$ iron-overload mice compared to WT controls.  $Tfr2^{mut/mut}$  and  $Hfe^{-f}$  mice had 3- and 3.5-fold increases in non-haem iron levels in the liver compared to WT controls, respectively (Figure 1A,C), thus confirming iron overload. Importantly, lung iron levels were significantly increased 1.5- and 0.75-fold in  $Tfr2^{mut/mut}$  and  $Hfe^{-f}$  mice compared to their controls, respectively (Figure 1A,C). We did not observe any compensatory increase in the expression of Tfr1 in  $Tfr2^{mut/mut}$ mice (supplementary material, Figure S1). DAB-enhanced Perls' iron staining showed that  $Tfr2^{mut/mut}$  and  $Hfe^{-f}$  mice exhibited iron accumulation predominantly in the airway basement membrane, blood vessels, and tissue macrophages (Figure 1B,D). Significantly, we found that  $Tfr2^{mut/mut}$  and  $Hfe^{-t}$  mice had significantly increased collagen deposition around the small airways compared to WT controls (Figure 1E,F), demonstrating that increased iron accumulation in the lungs was associated with increased airways fibrosis.

# *Tfr2<sup>mut/mut</sup>* and *Hfe<sup>-/-</sup>* mice have impaired lung function

Impaired lung function is the critical functional issue in respiratory diseases. Impaired lung function in respiratory disease is often associated with structural changes such as increased airways fibrosis that correlate with lung function decline. Thus, we examined next whether the structural changes observed in iron overload mice are associated with impaired lung function. We found that  $Tfr2^{mut/mut}$  mice had a trend (p=0.07) towards increased baseline central airways resistance (Rn), but no changes in transpulmonary resistance (Rrs), compliance (Crs) or elastance (Ers) compared to WT controls (Figure 2A–C and supplementary material, Figure S2A).  $Hfe^{-f}$  mice had increased baseline Rrs and Ers and decreased Crs (Figure 2D–F and supplementary material, Figure S2B). Significantly, both  $Tfr2^{mut/mut}$  and  $Hfe^{-f}$  mice had altered lung function, characterised by increased Rn, Rrs, and Ers, and decreased Crs in response to nebulised methacholine (MCh) (Figure 2A–F and supplementary material, Figure S2A,B). Thus, iron accumulation in the lung was associated with significant deterioration of lung function.

We assessed the possibility that the functional changes observed with iron overload were driven by altered smooth muscle contraction by measuring airway contractility in precision cut lung slices (PCLS). Each slice was perfused with increasing concentrations of methacholine (MCh) (0.001–1  $\mu$ M) and the contractile response measured for each concentration. MCh induced concentration-dependent contraction of small airways in both WT and *Tfr2<sup>mut/mut</sup>* mice (Figure 2G), but there were no differences in maximum percentage reduction in lumen area between the two groups (50.7 ± 7.0% versus 56.4 ± 8.5%). These data suggest that increased lung iron does not increase airway smooth muscle contractility.

# Immune and inflammatory responses are not considerably increased in $Tfr2^{mut/mut}$ and $Hfe^{-t}$ mice

We next assessed immune factor (*Tlr2*, *Tlr4*, *Il6*, *Il1β*, *Tnfα*, *Ho1*) expression and BALF cell levels in the lungs of  $Tfr2^{mut/mut}$  and  $Hfe^{-/-}$  mice compared to WT controls (supplementary material, Figure S3). Despite alterations in lung function, only *Il1β* and *Ho1* expression were increased in  $Tfr2^{mut/mut}$  mice (supplementary material, Figure S3A). Neither  $Tfr2^{mut/mut}$  nor  $Hfe^{-/-}$  mice had increased inflammatory cell numbers in BALF (supplementary material, Figure S3A,B). These data suggest that iron overload is not associated with substantial increases in immune and/or inflammatory responses.

Collectively, our data supports that iron-associated changes in lung function do not result from increased inflammation (supplementary material, Figure S3) or airway smooth muscle contractility but rather structural changes (i.e. small airways fibrosis).

# Bleomycin-induced pulmonary fibrosis is associated with increased iron levels and altered expression of iron-related genes

Since increased iron has been linked with fibrotic lung diseases, including IPF, and since we show that mice with increased lung iron levels have increased fibrosis in the absence of other disease-associated- and/or inducing-stimuli, we explored the role of increased iron in IPF using complementary experimental and human analyses.

Bleomycin-induced experimental pulmonary fibrosis is widely used to help determine the mechanisms of pathogenesis, and test therapies for, fibrotic lung disease in humans. We assessed systemic and pulmonary iron levels, iron-related gene expression, lung tissue remodelling and lung function in a bleomycin-induced model of experimental pulmonary fibrosis. We found that, in the absence of bleomycin treatment, sham (PBS)-treated,  $Tfr2^{mut/mut}$ 

mice had significantly increased iron levels in both the lung and liver compared to WT controls (Figure 3A). Bleomycin-treated (d28 post treatment) WT mice had increased non-haem iron levels in the lung, but not in the liver, compared to sham-treated WT mice, with levels similar to that observed in PBS-treated  $Tfr2^{mut/mut}$  mice. This demonstrates that bleomycin treatment increased iron levels in the lung to the same extent as that observed in sham-treated  $Tfr2^{mut/mut}$ mice. Interestingly, bleomycin-treated Tfr2<sup>mut/mut</sup> mice had similar lung iron levels as shamtreated Tfr2<sup>mut/mut</sup> and bleomycin-treated WT controls (Figure 3A). Iron accumulation localised predominantly to macrophages (based on cellular morphology) following bleomycin treatment (Figure 3B). Compared to sham-treated WT mice, *Tfr2<sup>mut/mut</sup>* mice had increased mRNA levels for the divalent metal transporter 1 (Dmt1-ire, Slc11a2) and zinc transporter (Zip14) in whole lung tissues (Figure 3C). In addition, bleomycin-treated WT mice had increased mRNA levels for ferritin heavy chain (*Fth*) and decreased expression of *Dmt1-ire*, *Tfr1*, *Zip14*, iron regulatory protein 1 (Irp1), hepcidin (Hamp), and ceruloplasmin (Cp) in the lung compared to sham-treated WT controls (Figures 3C). With the exception of *Fth*, which was decreased, there were no other changes in iron-related gene expression in bleomycin-treated  $Tfr2^{mut/mut}$  mice compared to bleomycin-treated WT controls. Taken together, these findings show that bleomycin-induced pulmonary fibrosis is characterised by increased iron accumulation in the lung, similar to that in the TFR2<sup>mut/mut</sup> model of iron overload, and is associated with significant evidence of altered iron-related gene expression.

# Increased iron accumulation in $Tfr2^{mut/mut}$ mice is associated with increased fibrosis in bleomycin-induced experimental pulmonary fibrosis

We assessed the role of lung iron overload on airway fibrosis and lung function in  $Tfr2^{mut/mut}$  mice with and without bleomycin treatment (d28 post treatment). In the absence of bleomycin treatment,  $Tfr2^{mut/mut}$  mice had increased small airways fibrosis compared to WT controls (Figure 3D). Importantly, the magnitude of small airway fibrosis in  $Tfr2^{mut/mut}$  mice in the

absence of bleomycin treatment was similar to that in bleomycin-treated WT controls. Interestingly, bleomycin-treated,  $Tfr2^{mut/mut}$  mice had increased pulmonary tissue density of collagen, Ashcroft score and small airways fibrosis compared to bleomycin-treated WT controls (Figure 3D, E). Similarly, in the absence of bleomycin,  $Tfr2^{mut/mut}$  mice had increased Rn and Rrs in response to MCh (30 mg/ml) compared to sham-treated WT controls, with the magnitude being similar to that in bleomycin-treated WT groups (Figure 3F). Whilst bleomycin-treated,  $Tfr2^{mut/mut}$  mice had increased small airways fibrosis compared to bleomycin-treated WT controls, with the magnitude being similar to that in bleomycin-treated WT groups (Figure 3F). Whilst bleomycin-treated WT controls (Figure 3D), bleomycin had no additional effects on lung function in  $Tfr2^{mut/mut}$  mice (Figure 3F and supplementary material, Figure S4). Taken together these findings support that increased iron in the lung plays an important role in driving airway fibrosis in bleomycin-induced experimental pulmonary fibrosis.

# Iron levels increase in the later stages of bleomycin-induced pulmonary fibrosis and correspond with small airways fibrosis and reduced gas exchange

We investigated iron levels and small airway fibrosis and gas exchange (DF<sub>CO</sub>) at different time points (d2, 7, and 22) following bleomycin treatment in WT mice. Treatment has no effect on liver iron levels at any time point (Figure 4A). Significantly, whilst no significant changes in iron accumulation in the lung during the early stages post-treatment, iron levels increase in the lung of bleomycin-treated mice compared to sham-treated controls by day 22 (Figure 4A). This increase in iron level corresponds with the development of small airway fibrosis and a decline in DF<sub>CO</sub> (Figures 4B,C). These data provide a link between increased pulmonary iron accumulation and progression of fibrosis and lung function decline in experimental pulmonary fibrosis.

Iron levels are increased in the lung tissues of patients with IPF, and exogenous iron increases human lung fibroblast proliferation and cytokine and ECM responses To validate our experimental findings in human disease and to investigate potential mechanisms, we measured iron levels in lung biopsies from IPF patients and healthy controls. Iron accumulation was significantly increased in the lung tissues of IPF patients compared to healthy controls (Figure 5A). Importantly, iron accumulation negatively correlates with FVC% predicted (Figure 5B). A trend towards a negative correlation between FEV1% predicted and iron accumulation was also observed (Figure 5C). To assess the potential effects of increased iron accumulation on fibrotic responses, human lung fibroblasts were cultured in the presence of a water-soluble iron salt, ferric ammonium citrate (FAC), at 10 or 50  $\mu$ M. FAC increased cellular proliferation (Figure 5D), and the expression of IL6 and IL8 (Figure 5E). FAC at 10  $\mu$ M also increased the mRNA levels of the ECM genes *COL1A2* and *TNC* (Figure 5F). Taken together these findings showed that iron levels were substantially increased in the lungs of IPF patients, and that increased accumulation of iron in the lungs may promote the pathogenesis of IPF by increasing the proliferation of, and cytokine and ECM production by, lung fibroblasts.

# Iron chelator treatment ameliorates fibrotic lung disease in bleomycin-induced pulmonary fibrosis

We assessed the therapeutic potential of targeting the increased iron accumulation that occurs in fibrotic disease. WT BALB/c mice were treated daily with the iron chelator, DFO, from day 14 following administration of bleomycin, which is before iron increases and disease features emerge (Figure 4), until day 27. The effects of treatment on key features of disease were assessed on day 28. Bleomycin-treated WT mice had increased total leukocytes, macrophages, lymphocytes, neutrophils, and eosinophils in their BALF compared to sham-treated controls (Figure 6A). DFO treatment markedly suppressed these inflammatory responses. Bleomycin-treated mice had increased levels of collagen deposition around the small airways, higher Ashcroft scores and more hydroxyproline in their lungs; these increases were suppressed by DFO treatment (Figure 6B,C). We also show that bleomycin-treated mice had suppressed

(~10%) gas exchange and DFco compared to sham-treated controls, and that DFO administration prevented these declines (Figure 6D). We also found that DFO treatment suppressed MCh-induced AHR, in terms of Rn, Rrs and Ers, in bleomycin-induced pulmonary fibrosis (Figure 6E). These findings demonstrated that DFO treatment protects against the progression of fibrosis and decline in lung function in bleomycin-induced experimental pulmonary fibrosis. Interestingly, DFO treatment in the absence of bleomycin-induced pulmonary fibrosis resulted in a small increase in Ashcroft score and decrease in DFco (Figure 6C,D). Taken together these data reinforce the important role of iron in the pathogenesis of fibrotic lung disease and demonstrate the therapeutic potential for targeting increased pulmonary iron in preventing/treating disease progression, whilst also highlighting that the manipulation of iron may also have detrimental effects in the lung.

We sought to determine whether bleomycin-associated iron accumulation in the lung affects Tfr1<sup>+</sup> macrophage number and phenotype as has been observed in IPF by Allden *et al.* (2). We found that Tfr1<sup>+</sup> cell abundance increased in bleomycin-treated mice and that these cells were predominantly macrophages (Figure 6F). Interestingly, we found that DFO treatment results in a reduction in these Tfr1<sup>+</sup> cells (Figure 6F). These data suggest that bleomycin treatment results in an accumulation of macrophages with the ability to sequester iron, and DFO treatment-induced suppression of disease is associated with a reduction in the–abundance of these cells. To determine whether these Tfr1<sup>+</sup> macrophage populations display altered phenotypes, we measured expression of a range of M1-like (*Ifng, Tlr2, Marco, Inos*) and M2-like (*Arg1, Il10, Timp1, Mmp9*) phenotypic gene signatures in sorted Tfr1<sup>+</sup> and Tfr1<sup>-</sup> macrophages in the presence or absence of bleomycin-induced pulmonary fibrosis treatment. We found that Tfr1<sup>+</sup> macrophages from saline-treated mice showed lower expression levels of *Tlr2* and *Mmp9* and a higher level of *Il10* compared to Tfr1<sup>-</sup> macrophages from saline-treated controls (Figure 6G). This supports that, in the absence of disease, Tfr1<sup>+</sup> macrophages have an anti-inflammatory M2-like phenotype which has been shown to be associated with tissue repair

responses, while Tfr1<sup>-</sup> macrophages appear to have a greater pro-inflammatory M1-like phenotype. Importantly, Tfr1<sup>+</sup> macrophages from bleomycin-treated mice had increased Arg1, *Ill0*, and *Timp1* expression compared to Tfr1<sup>+</sup> macrophages, from saline treated controls suggestive of a more M2-like phenotype for Tfr1<sup>+</sup> macrophages in pulmonary fibrosis (Figure 6G). This is important because M2-like macrophages have been shown to play important roles in initiating proliferative tissue repair processes and fibrosis [28]. Interestingly, we also found that Tfr1<sup>+</sup> macrophages from mice with bleomycin-induced pulmonary fibrosis mice had decreased Mmp9, Tlr2, Marco (p=0.06), but increased Il10 and Ifng expression compared to Tfr1<sup>-</sup> macrophages from these mice (Figure 6G and supplementary material, Figure S5), which suggests that Tfr1<sup>+</sup> macrophages likely play a different role in disease with a phenotype that has both M1- and M2-like properties. We also assessed iron-related gene signatures (Dmt1, Irp1, *Ftl*) in Tfr1<sup>+</sup> and Tfr1<sup>-</sup> macrophages and found that Tfr1<sup>+</sup> macrophages had decreased Dmt1 and Irpl expression compared to Tfr1<sup>-</sup> macrophages in the presence and absence of bleomycininduced pulmonary fibrosis (Figure 6G and supplementary material, Figure S5), suggesting that the Tfr1<sup>+</sup> macrophages have less iron accumulation. We also found that transferrin levels were not altered in the BAL collected from bleomycin-treated mice compared to controls (supplementary material, Figure S6). Taken together these data demonstrate that  $Tfr1^+$  and  $Tfr1^$ macrophages display complex phenotypes in bleomycin-induced pulmonary fibrosis and that more studies are required to determine the role of Tfr1<sup>+</sup> and Tfr1<sup>-</sup> macrophages in fibrotic lung disease, especially the effects that iron sequestration in these cells has on phenotype.

# Discussion

In this study we showed, for the first time, that elevated systemic iron levels in aged  $Tfr2^{mut/mut}$ and  $Hfe^{-/-}$  mice were associated with increased iron levels in the lung, and that this iron accumulation was associated with significant increases in airway fibrosis and altered lung function. These findings showed that increased iron accumulation in the lung was associated with increased airways fibrosis in the absence of noxious exogenous stimuli, thus highlighting that increased iron itself may play a role in the pathogenesis of key features of disease observed in fibrotic lung diseases such as IPF. Previous studies have shown increased iron accumulation in AMs in IPF patients [1,2] suggesting that iron metabolism is altered in disease. Furthermore, Allden *et al.*, have recently shown that that TFR1<sup>-</sup> AMs have a decreased ability to sequester iron, that the proportion of TFR1-negative AMs is reduced in IPF patient and that this reduction is associated with increased BAL transferrin levels and poorer disease prognosis [2]. Our findings expand upon these clinical data and suggest that changes in the number of iron sequestering TFR1<sup>+</sup> macrophages are a feature of disease in whole lung tissue, and that the capability to control increases in pulmonary iron by these cells, and/or a change in their phenotype that results from iron sequestration, in IPF may play a role in the development of disease.

We found that iron accumulation was increased in lung tissue sections from patients with IPF and in experimental bleomycin-induced pulmonary fibrosis. Furthermore, we found that the increasing iron levels in bleomycin-induced pulmonary fibrosis corresponded with the development of airway fibrosis and a decline in lung function and that the administration of exogenous iron increases cellular proliferation and pro-inflammatory cytokine and extracellular matrix gene expression in human lung fibroblasts. Fibrosis, associated with the deposition of collagen and other ECM proteins, is an important pathological manifestation and key feature of IPF, asthma and COPD [29-32]. Collagen is the most abundant ECM protein in the body [33]. Previous reports show that excess iron levels are associated with higher activity of prolyl hydroxylase (a key enzyme involved in collagen synthesis) and collagen deposition in the liver [34,35]. Iron affects enzyme function in normal collagen synthesis and plays a vital role in collagen maturation [36,37]. In our study, we extended these findings by showing that increased iron levels can directly increase the proliferation and pro-inflammatory cytokine and ECM responses of human lung fibroblasts. These findings provide strong evidence that increased

levels of iron in the lung in IPF, perhaps as a result of decreased iron sequestration by AMs [2], may promote the pathogenesis of fibrosis by increasing pro-inflammatory cytokine production and/or ECM deposition by lung fibroblasts.

Bleomycin complexes with host iron and subsequently generates free radicals, which cause DNA damage that initiates experimental pulmonary fibrosis [38-40]. Previous studies have shown reduced fibrosis when DFO treatment occurs during the initial bleomycin administration and then throughout the development of bleomycin-induced pulmonary fibrosis [41-43]. Our data showed that, in WT mice, the accumulation of iron occurs long after the initial bleomycin insult and that features of disease emerge in association with increased iron levels. We also showed that  $Tfr2^{mut/mut}$  mice not treated with bleomycin have similar disease features as WT mice treated with bleomycin and that bleomycin treatment in  $Tfr2^{mut/mut}$  mice does not result in a synergistic increase in features of disease compared to that observed in sham-treated  $Tfr2^{mut/mut}$  controls. Taken together, these data support that an accumulation of iron in the lung, rather than iron status at the time of bleomycin treatment, drive disease. To confirm the role, and the potential for therapeutically-reducing the effects of iron accumulation in bleomycin-induced pulmonary fibrosis, we used DFO to counter the effects of iron accumulation. DFO allowed us to examine the role of iron accumulation and also test whether we could target iron as a therapy. We treated WT BALB/c mice intranasally with DFO daily from 14–27 days after bleomycin exposure. We chose this protocol because we found that iron levels increase, and pulmonary fibrosis emerges, 14-22 days after bleomycin treatment. Significantly, we found that this iron chelator therapy completely suppresses key features of pulmonary fibrosis, even when treatment occurs well after the initial bleomycin challenge and, importantly, when iron levels increase in association with the emergence of disease. Interestingly, we also found that DFO reduces the number of Tfr1<sup>+</sup> macrophages in bleomycininduced pulmonary fibrosis. Because we showed that these cells have a more M2-like phenotype, and because M2-like macrophages have been shown to play an important role in

fibrosis [44], our data support that DFO may have effects through its ability to alter the abundance of these cells in disease. However, since we also found that Tfr1<sup>+</sup> macrophages have a gene expression profile that may have protective effects in fibrosis (reduced Mmp9 and increased Timp1), our findings suggest that more studies are required to determine the role of these cells in disease. In addition to its iron-chelating ability, DFO has antioxidant and freeradical scavenging properties that could have suppressed manifestations of bleomycin-induced lung fibrosis through reducing oxidative stress and associated pathological responses [45]. It is also possible that DFO could activate the hypoxia-inducible factor signalling pathway, which could have suppressed the features of bleomycin-induced lung fibrosis [46]. It is well known that iron needs to be tightly controlled with evidence for dysregulation in either direction known to result in pathology (1). In our studies we found that despite DFO having substantial protective effects in a murine model of bleomycin-induced pulmonary fibrosis, DFO treatment in the absence of bleomycin resulted in small changes in Ashcroft score and DFco (Figure 6C, D). These data highlight the fact that DFO is a crude tool for modifying iron and support the premise that iron regulation is extremely complex with much work still required to identify effective iron-targeted therapies that do not have pathological consequences.

In conclusion, our findings demonstrated that an endogenous increase in iron levels in the lungs drives key features of lung disease, most notably fibrosis. We further showed that iron levels are increased and play an important role in the progression of experimental and clinical fibrotic lung disease and that this may be a result of increased iron-induced activation of lung fibroblasts. Significantly, we showed that targeting increased iron accumulation, that has been shown to occur in progressive fibrotic lung diseases, such as IPF, by us and others, may be an effective therapeutic strategy for the prevention and/or treatment of disease.

### Acknowledgements

This work was supported by grants and fellowships from the Cystic Fibrosis Australia and the Australian Cystic Fibrosis Research Trust and The University of Newcastle, Australia. PMH and DT are funded by Fellowships from the NHMRC (1079197 and 1020437). JKB was supported by a University of Groningen/European Union Rosalind Franklin Fellowship.

# Author contributions statement

MKA, RYK, ACB, AP and JCH performed most of the mouse experiments and analysed data. MKA, RYK, DJ, EAM, PMH and JCH conceptualized and designed studies, analysed and interpreted data, wrote and edited the manuscript. DT provided the genetic iron overload mouse models. TB and JKB performed staining and analysis of clinical IPF samples. DX and BO performed and analysed human fibroblast experiments. CD, GL, BF, JWP, JRM, ACB, RA, AP, KSV, RK, MH and KLM assisted in performing specific techniques associated with mouse experiments and/or iron assessment(s). RYK, DMJ, EAM, PMH and JCH supervised the studies. All authors participated in the interpretation of data, preparation and editing of manuscript for intellectual content. All authors read and approved the final manuscript.

# Data availability statement

The data that support the findings of this study are available from the corresponding author JCH, upon reasonable request.

# References

- Ali MK, Kim RY, Karim R, *et al.* Role of iron in the pathogenesis of respiratory disease. *Int J Biochem Cell Biol* 2017; 88: 181–195.
- Allden SJ, Ogger PP, Ghai P, *et al.* The Transferrin Receptor CD71 delineates functionally distinct airway macrophage subsets during idiopathic pulmonary fibrosis. *Am J Respir Crit Care Med* 2019; **200**: 209–219.
- 3. Giorgi G, D'Anna MC, Roque ME. Iron homeostasis and its disruption in mouse lung in iron deficiency and overload. *Exp Physiol* 2015; **100:** 1199–1216.
- Neves J, Leitz D, Kraut S, *et al.* Disruption of the hepcidin/ferroportin regulatory system causes pulmonary iron overload and restrictive lung disease. *EBioMedicine* 2017; 20: 230– 239.
- Toblli JE, Cao G, Giani JF, *et al.* Markers of oxidative/nitrosative stress and inflammation in lung tissue of rats exposed to different intravenous iron compounds. *Drug Des Devel Ther* 2017; 11: 2251–2263.
- 6. Fleming RE, Ahmann JR, Migas MC, *et al.* Targeted mutagenesis of the murine transferrin
  receptor-2 gene produces hemochromatosis. *Proc Natl Acad Sci U S A* 2002; 99: 10653–10658.
- Zhou XY, Tomatsu S, Fleming RE, *et al.* HFE gene knockout produces mouse model of hereditary hemochromatosis. *Proc Natl Acad Sci U S A* 1998; 95: 2492–2497.
- Liu G, Cooley MA, Jarnicki AG, *et al.* Fibulin-1 regulates the pathogenesis of tissue remodeling in respiratory diseases. *JCI Insight* 2016; 1: e86380.
- Gold MJ, Hiebert PR, Park HY, *et al.* Mucosal production of uric acid by airway epithelial cells contributes to particulate matter-induced allergic sensitization. *Mucosal Immunol* 2016;
   9: 809–820.

- Johnstone D, Milward EA. Genome-wide microarray analysis of brain gene expression in mice on a short-term high iron diet. *Neurochem Int* 2010; 56: 856–863.
- Heidari M, Johnstone DM, Bassett B, *et al.* Brain iron accumulation affects myelin-related molecular systems implicated in a rare neurogenetic disease family with neuropsychiatric features. *Mol Psychiatry* 2016; **21:** 1599–1607.
- Horvat JC, Beagley KW, Wade MA, *et al.* Neonatal chlamydial infection induces mixed Tcell responses that drive allergic airway disease. *Am J Respir Crit Care Med* 2007; **176:** 556– 564.
- 13. Horvat JC, Starkey MR, Kim RY, *et al.* Chlamydial respiratory infection during allergen sensitization drives neutrophilic allergic airways disease. *J Immunol* 2010; **184:** 4159–4169.
- Hübner R-H, Gitter W, El Mokhtari NE, *et al.* Standardized quantification of pulmonary fibrosis in histological samples. *Biotechniques* 2008; 44: 507–511, 514–507.
- 15. Starkey MR, Nguyen DH, Brown AC, *et al.* Programmed Death Ligand 1 promotes early-life chlamydia respiratory infection-induced severe allergic airway disease. *Am J Respir Cell Mol Biol* 2016; **54**: 493–503.
- 16. Kim RY, Pinkerton JW, Essilfie AT, *et al.* Role for NLRP3 inflammasome-mediated, IL1beta-dependent responses in severe, steroid-resistant asthma. *Am J Respir Crit Care Med* 2017; **196**: 283–297.
- Limjunyawong N, Mitzner W, Horton MR. A mouse model of chronic idiopathic pulmonary fibrosis. *Physiol Rep* 2014; 2: e00249.
- Fallica J, Das S, Horton M, *et al.* Application of carbon monoxide diffusing capacity in the mouse lung. *J Appl Physiol (1985)* 2011; **110:** 1455–1459.
- Kim RY, Horvat JC, Pinkerton JW, *et al.* MicroRNA-21 drives severe, steroid-insensitive experimental asthma by amplifying phosphoinositide 3-kinase-mediated suppression of histone deacetylase 2. *J Allergy Clin Immunol* 2017; **139:** 519–532.

- 20. Horvat JC, Starkey MR, Kim RY, et al. Early-life chlamydial lung infection enhances allergic airways disease through age-dependent differences in immunopathology. J Allergy Clin Immunol 2010; 125: 617–625.e6.
- 21. Donovan C, Royce SG, Esposito J, *et al.* Differential effects of allergen challenge on large and small airway reactivity in mice. *PLoS One* 2013; **8:** e74101.
- 22. Bourke JE, Bai Y, Donovan C, *et al.* Novel small airway bronchodilator responses to rosiglitazone in mouse lung slices. *Am J Respir Cell Mol Biol* 2014; **50**: 748–756.
- 23. Donovan C, Bailey SR, Tran J, *et al.* Rosiglitazone elicits in vitro relaxation in airways and precision cut lung slices from a mouse model of chronic allergic airways disease. *Am J Physiol Lung Cell Mol Physiol* 2015; **309:** L1219–1228.
- 24. Donovan C, Seow HJ, Bourke JE, *et al.* Influenza A virus infection and cigarette smoke impair bronchodilator responsiveness to beta-adrenoceptor agonists in mouse lung. *Clin Sci* (*Lond*) 2016; **130**: 829–837.
- 25. Clifford RL, Fishbane N, Patel J, *et al.* Altered DNA methylation is associated with aberrant gene expression in parenchymal but not airway fibroblasts isolated from individuals with COPD. *Clin Epigenetics* 2018; **10:** 32.
- 26. Ong J, Timens W, Rajendran V, *et al.* Identification of transforming growth factor-betaregulated microRNAs and the microRNA-targetomes in primary lung fibroblasts. *PLoS One* 2017; **12:** e0183815.
- Krimmer D, Ichimaru Y, Burgess J, *et al.* Exposure to biomass smoke extract enhances fibronectin release from fibroblasts. *PLoS One* 2013; 8: e83938.
- Wynn TA, Vannella KM. Macrophages in tissue repair, regeneration, and fibrosis. *Immunity* 2016; 44: 450–462.
- 29. Chakir J, Shannon J, Molet S, *et al.* Airway remodeling-associated mediators in moderate to severe asthma: effect of steroids on TGF-beta, IL-11, IL-17, and type I and type III collagen expression. *J Allergy Clin Immunol* 2003; **111:** 1293–1298.

- Dolhnikoff M, da Silva LF, de Araujo BB, *et al.* The outer wall of small airways is a major site of remodeling in fatal asthma. *J Allergy Clin Immunol* 2009; **123**: 1090–1097.e1.
- 31. Haw TJ, Starkey MR, Pavlidis S, *et al.* Toll-like receptor 2 and 4 have opposing roles in the pathogenesis of cigarette smoke-induced chronic obstructive pulmonary disease. *Am J Physiol Lung Cell Mol Physiol* 2017; **314:** L298–L317.
- 32. Liu G, Cooley MA, Nair PM, *et al.* Airway remodelling and inflammation in asthma are dependent on the extracellular matrix protein fibulin-1c. *J Pathol* 2017; **243:** 510–523.
- Shoulders MD, Raines RT. Collagen structure and stability. *Annu Rev Biochem* 2009; 78: 929–958.
- 34. Pietrangelo A, Gualdi R, Casalgrandi G, *et al.* Molecular and cellular aspects of iron-induced hepatic cirrhosis in rodents. *J Clin Invest* 1995; **95:** 1824–1831.
- 35. Irving MG, Booth CJ, Devlin CM, *et al.* The effect of iron and ethanol on rat hepatocyte collagen synthesis. *Comp Biochem Physiol C* 1991; **100:** 583–590.
- 36. Prockop DJ. Role of iron in the synthesis of collagen in connective tissue. *Fed Proc* 1971;30: 984–990.

ente

- 37. Tuderman L, Myllyla R, Kivirikko KI. Mechanism of the prolyl hydroxylase reaction. 1. Role
  of co-substrates. *Eur J Biochem* 1977; 80: 341–348.
- Kobayashi T, Guo LL, Nishida Y. Mechanism of double-strand DNA cleavage effected by iron-bleomycin. *Z Naturforsch C* 1998; 53: 867–870.
- Antholine WE, Petering DH, Saryan LA, *et al.* Interactions among iron(II) bleomycin, Lewis bases, and DNA. *Proc Natl Acad Sci U S A* 1981; 78: 7517–7520.
- Burger RM, Peisach J, Blumberg WE, *et al.* Iron-bleomycin interactions with oxygen and oxygen analogues. Effects on spectra and drug activity. *J Biol Chem* 1979; 254: 10906–10912.
- 41. Chandler DB, Butler TW, Briggs DD, 3rd, *et al.* Modulation of the development of bleomycin-induced fibrosis by deferoxamine. *Toxicol Appl Pharmacol* 1988; **92:** 358–367.

- 42. Chandler DB, Fulmer JD. The effect of deferoxamine on bleomycin-induced lung fibrosis in the hamster. *Am Rev Respir Dis* 1985; **131:** 596–598.
- 43. Kennedy JI, Chandler DB, Jackson RM, *et al.* Reduction in bleomycin-induced lung hydroxyproline content by an iron chelating agent. *Chest* 1986; **89:** 123S–125S.
- 44. Hou J, Shi J, Chen L, *et al.* M2 macrophages promote myofibroblast differentiation of LR-MSCs and are associated with pulmonary fibrogenesis. *Cell Commun Signal* 2018; **16**: 89.
- 45. Morel I, Cillard J, Lescoat G, *et al.* Antioxidant and free radical scavenging activities of the iron chelators pyoverdin and hydroxypyrid-4-ones in iron-loaded hepatocyte cultures: comparison of their mechanism of protection with that of desferrioxamine. *Free Radic Biol Med* 1992; **13**: 499–508.
- Chen Y, Gao S, Yan Y, *et al.* Aerosolized deferoxamine administration in mouse model of bronchopulmonary dysplasia improve pulmonary development. *Am J Transl Res* 2018; 10: 325–332.
- \*47. Hansbro PM, Hamilton MJ, Fricker M, *et al.* Importance of mast cell Prss31/transmembrane tryptase/tryptase-gamma in lung function and experimental chronic obstructive pulmonary disease and colitis. *J Biol Chem* 2014; **289:** 18214–18227.
- 48 Fricker M, Goggins BJ, Mateer S, *et al.* Chronic cigarette smoke exposure induces systemic hypoxia that drives intestinal dysfunction. *JCI Insight* 2018; **3:** e94040.
- \*49 Essilfie AT, Horvat JC, Kim RY, *et al.* Macrolide therapy suppresses key features of experimental steroid-sensitive and steroid-insensitive asthma. *Thorax* 2015; **70:** 458–467.
- \*50 Asquith KL, Horvat JC, Kaiko GE, *et al.* Interleukin-13 promotes susceptibility to chlamydial infection of the respiratory and genital tracts. *PLoS Pathog* 2011; **7:** e1001339.

\*Cited only in supplementary material.

ccepted Artic

**Figure 1.** Iron levels in the lungs of  $Tfr2^{mut/mut}$  and  $Hfe^{-t}$  mice. (A, C) Non-haem iron (NHI) levels were measured in liver and lung tissue of  $Tfr2^{mut/mut}$  (n=7) and  $Hfe^{-t}$  mice (n=12) and wild type (WT) controls (n=4-6). (B, D) Localisation of iron in lung sections using DAB-enhanced Perls' iron stain. (E, F) Area of collagen deposition surrounding the basement membrane of small airways was quantified in Sirius Red-stained lung tissue sections from  $Tfr2^{mut/mut}$  (n=7), and  $Hfe^{-t}$  mice (n=12) and wild type (WT) controls (n=4-6), in 6–8 airways/mouse. Representative images of collagen deposition around small airways at 40x objective. Mean  $\pm$  SEM. \*p<0.05, \*\*p<0.01, \*\*\*p<0.001, \*\*\*p<0.001.

**Figure 2.**  $Tfr2^{mut/mut}$  and  $Hfe^{-t}$  mice have impaired lung function. (A–F) Lung function in terms of central airways resistance (Rn) and transpulmonary resistance (Rrs) and elastance (Ers) was measured at baseline and in response to increasing doses of nebulised methacholine (MCh) in  $Tfr2^{mut/mut}$  (*n*=7) and  $Hfe^{-t}$  mice (*n*=12) and wild type (WT) controls (*n*=4–6). Precision cut lung slices were prepared, and airway contractility were measured with increasing concentrations of methacholine in  $Tfr2^{mut/mut}$  mice (*n*=3) and WT controls (*n*=3) (G) Airway lumen area at different concentrations of MCh. Mean ± SEM. \**p*<0.05, \*\**p*<0.01, \*\*\*\**p*<0.0001.

**Figure 3.** Bleomycin-induced pulmonary fibrosis is associated with increased iron levels and altered iron-related gene expression in the lung, and increased tissue density, Ashcroft score and small airways fibrosis and reduced lung function.  $Tfr2^{mut/mut}$  mice or wild-type (WT) controls were challenged with bleomycin (Bleo) or PBS intranasally (WT PBS n=8,  $Tfr2^{mut/mut}$  PBS n=4, WT Bleo n=9,  $Tfr2^{mut/mut}$  n=6). (A) On day 28, mice were sacrificed, and lung and liver tissues were collected and non-haem iron (NHI) levels were measured in liver and lung tissues. (B) localisation of iron in lung tissue sections was assessed using DAB-enhanced Perls' iron

23

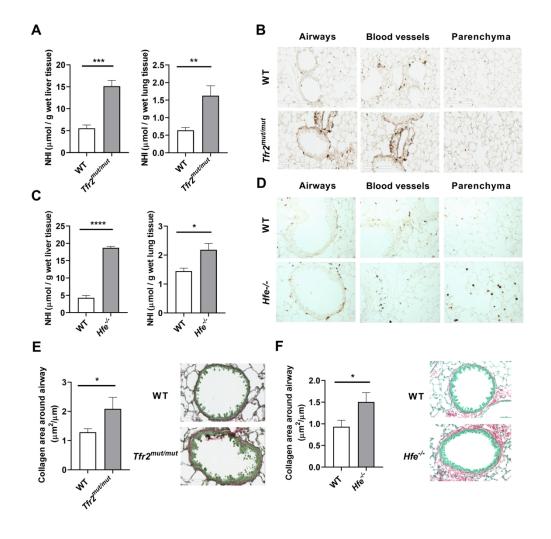
staining. (C) mRNA expression of the iron-related genes *Fth*, *Ftl*, *Dmt1-ire*, *Tfr1*, *Zip14*, *Irp1* and *2*, *Hamp*, and *Cp* was assessed by RT-qPCR) in whole lung homogenates relative to *Hprt*. (D) Collagen area around the small airways in Picro Sirius red-stained lung sections (6–8 airways/mouse) assessed using ImageJ analysis software. Representative images at 40x objective. (E) Tissue density and Ashcroft score was assessed in Picro Sirius red-stained lung sections. (F) Lung function in terms of central airways (Rn) and transpulmonary resistance (Rrs) and elastance (Ers) was measured in response to increasing doses of nebulised methacholine (MCh). Mean  $\pm$  SEM. \**p*<0.05, \*\**p*<0.01, \*\*\**p*<0.001, \*\*\**p*<0.0001.

**Figure 4.** Iron levels in the late stages of bleomycin-induced pulmonary fibrosis with increased iron corresponding with small airway fibrosis and reduced gas exchange. WT BALB/c mice were challenged with bleomycin (Bleo) or PBS intranasally (n=4-6/group). (A) Non-haem iron (NHI) levels in the liver and lung, (B) gas exchange in terms of diffusion fraction of carbon monoxide (DFco) and (C) small airway fibrosis were assessed on days 2, 7 and 22. Mean ± SEM. \*p<0.05, \*\*p<0.01, \*\*\*\*p<0.0001.

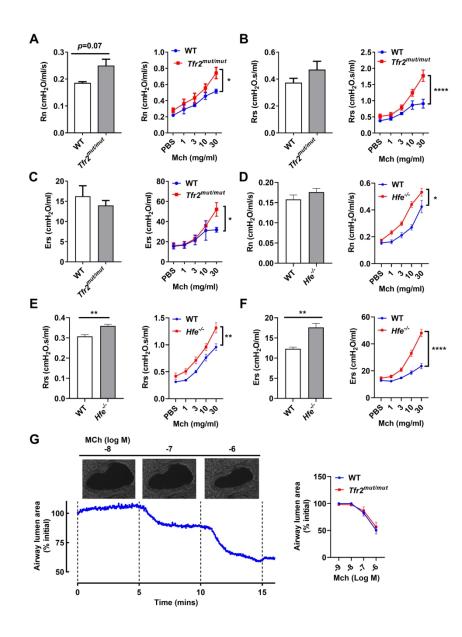
**Figure 5.** Iron levels are increased in the lung tissues of patients with IPF and iron increases human lung fibroblast proliferation and cytokine and ECM responses. Lung biopsy tissues were collected from IPF patients (*n*=10) and healthy controls (*n*=10). (A) Lung sections were stained with DAB-enhanced Perls' iron staining and iron levels were quantified by assessing staining intensity (n=10) using ImageJ software. (B, C) Human lung fibroblasts were cultured in the presence of ferric ammonium citrate (FAC; 10 or 50  $\mu$ M) or 0.1 BSA vehicle. Iron accumulation was correlated with FVC% predicted and FEV1% predicted. (D) Cellular proliferation was assessed using an MTT assay. (E) Effects of FAC on interleukin (IL)-6 and IL-8 release and (F) *COL1A2* and *TNC* mRNA levels. Mean ± SEM except for expression data presented as fold-change from matched control cultures. \**p*<0.05, \*\**p*<0.01.

Figure 6. Treatment with an iron chelator ameliorates fibrotic lung disease in bleomycininduced pulmonary fibrosis. WT BALB/c mice were challenged with bleomycin (Bleo) or PBS intranasally. Deferoxamine (DFO; 10 mg/kg) was administered intranasally daily to Bleo-treated mice on days 14-27. (A) On day 28, airway inflammation was quantified in terms of total leukocytes, macrophages, lymphocytes, neutrophils, and eosinophils per ml of BALF (Sal/PBS n=6, Bleo/PBS n=8, Bleo/DFO n=9, Sal/DFO n=4). Collagen deposition was assessed in Picro Sirius red-stained lung sections. (B) Collagen area around the small airways was measured in 6-8 airways/mouse (Sal/PBS n=6, Bleo/PBS n=8, Bleo/DFO n=9, Sal/DFO n=4) using ImageJ software. (C) Ashcroft score and hydroxyproline levels were assessed in the lung (Sal/PBS n=12, Bleo/PBS n=5-13, Bleo/DFO n=5-8, Sal/DFO n=10). (D) The diffusing fraction of carbon monoxide (DFco) was determined (Sal/PBS n=6, Bleo/PBS n=7, Bleo/DFO n=7, Sal/DFO n=4). (E) Lung function in terms of central airways resistance (Rn) and transpulmonary resistance (Rrs) and elastance (Ers) was measured at baseline and in response to increasing doses of nebulised methacholine (MCh) (Sal/PBS n=6, Bleo/PBS n=12, Bleo/DFO n=12, Sal/DFO n=4). (F) Tfr1+ cells were sorted from the lung of bleomycin and saline treated mice (Sal/PBS n=6, Bleo/PBS n=6, Bleo/DFO n=6, Sal/DFO n=4). (G) Macrophages phenotypes, profibrotic and iron relation gene expressions were assessed by RT-qPCR) (Sal/PBS *n*=3, Bleo/PBS *n*=3, Bleo/DFO *n*=3, Sal/DFO *n*=3). Mean ± SEM. \**p*<0.05, \*\**p*<0.01, \*\*\**p*<0.001, \*\*\*\**p*<0.0001.

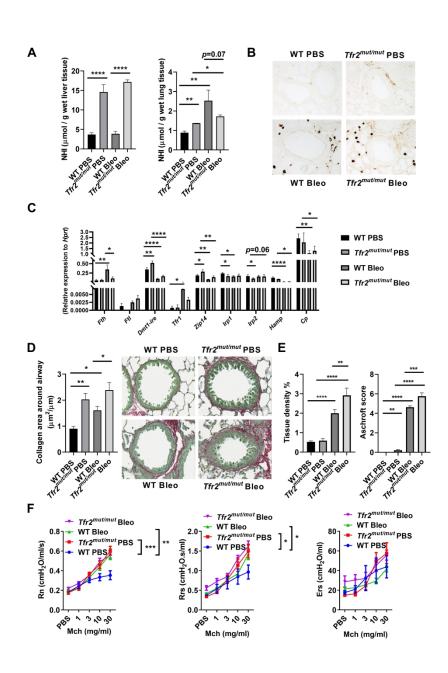
# rticle Accepte



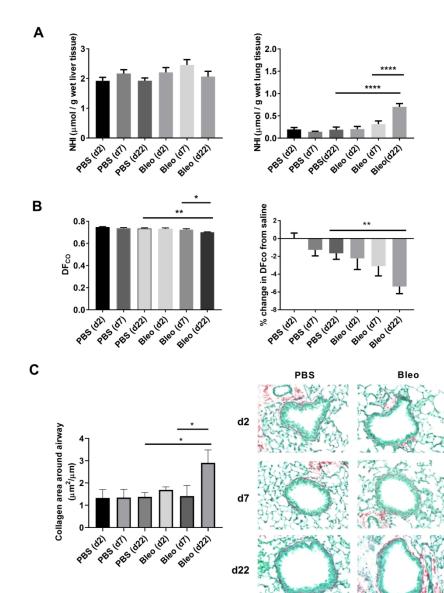
# rticle Accepte







# Iticle Accepte



# ticle Accepte

